J. Astrophys. Astr. (2019) 40:3
https://doi.org/10.1007/s12036-018-9568-8

The dynamic spectral signatures from lunar occultation: A simulation study

JIGISHA V. PATEL* and AVINASH A. DESHPANDE

Raman Research Institute, C. V. Raman Avenue, Sadashivanagar, Bengaluru 560 080, India.
*Corresponding author. E-mail: jigishapatel.7793@gmail.com

MS received 11 July 2018; accepted 28 November 2018

Abstract. Lunar occultation, which occurs when the Moon crosses sight-lines to distant sources, has been studied extensively through apparent intensity pattern resulting from Fresnel diffraction, and has been successfully used to measure angular sizes of extragalactic sources. However, such observations till date have been mainly over narrow bandwidth, or averaged over the observing band, and the associated intensity pattern in time has rarely been examined in detail as a function of frequency over a wide band. Here, we revisit the phenomenon of lunar occultation with a view to study the associated intensity pattern as a function of both time and frequency. Through analytical and simulation approach, we examine the variation of intensity across the dynamic spectra, and look for chromatic signatures which could appear as discrete dispersed signal tracks, when the diffraction pattern is adequately smoothed by a finite source size. We particularly explore circumstances in which such diffraction pattern might closely follow the interstellar dispersion law followed by pulsars and transients, such as the Fast Radio Bursts (FRBs), which remain a mystery even after a decade of their discovery. In this paper, we describe details of this investigation, relevant to radio frequencies at which FRBs have been detected, and discuss our findings, along with their implications. We also show how a *band-averaged* light curve suffers from temporal smearing, and consequent reduction in contrast of intensity variation, with increasing bandwidth. We suggest a way to recover the underlying diffraction signature, as well as the sensitivity improvement commensurate with usage of large bandwidths.

Keywords. Moon—occultation—ISM: general—radio continuum: general.

1. Introduction

An occultation takes place when a nearby celestial object moves in front of a distant one and blocks it from view. In early years, these observations in radio frequencies yielded measurements of diameters of small radio sources with accuracies much better than any other method available then, while requiring less instrumental efforts (Scheuer 1962; Von Hoerner 1963). The fluctuations in the received power when the Moon obstructs a radio source depends on the size of the source relative to the size of the Fresnel zone at the Moon's distance, which over the range of frequencies of interest, ranges from a few arc-second to a maximum of about 20 arc-second (Hazard *et al.* 1963; Hazard 1976; Scheuer 1962). Lunar occultation observations for about 1000 radio sources have been made with the steerable Ooty Radio Telescope at Ootacamund, India (Swarup *et al.* 1971; see also Singal 1987 and the references therein) However, all the findings so far used band averaged signatures of occultation light curves.

Here, we have attempted to find the spectral imprints of lunar occultation, which over a wide range of frequencies has not been explicitly studied yet. The intensity pattern due to Fresnel diffraction by straight edge for a range of frequencies depict spatial dispersion of fringes. This pattern sweeping across an observer, due to the motion of the moon relative to the sight-line to the source, manifests into temporal dispersion. Hence, the observed intensity profiles will show relative time delay that is correlated with frequency, when corresponding features at different radio frequencies are compared. The apparent pattern can be calculated using the standard formula for intensity at any point due to Fresnel diffraction by straight edge, resulting into dispersed dynamic spectrum. We have attempted to find if the dispersion signature observed follows a particular trend and explored the possibility of changes

Published online: 19 January 2019

in the trend under different circumstances. We have in particular explored the possibility of comparing it with the ISM dispersion law, followed by pulsars, FRBs (Lorimer *et al.* 2007) or similar pulsed signals.

In Section 2, we have first deduced a generic expression of intensity as function of frequency and distance, which is further utilized to find dispersion like delay and for simulating the spectral signatures. Further, we take into account few situations and observe the changes in the diffraction pattern, in turn the changes in dynamic spectrum and dispersion characteristics.

In Section 3, situations differing in assumptions of velocity of obstruction, source size and minimum distance to obstruction are considered. The dispersion delay and spectral signatures for above scenarios are analyzed using simulations. We have also tried to explore circumstances in which the dispersion trend found for diffraction closely follows the dispersion trend of ISM.

In Section 4, we discuss some key implications of wide bandwidth observations for signal-to-noise ratio improvement in estimation of the average intensity pattern and summarize our conclusions in the last section.

2. Spatial dispersion in Fresnel diffraction

An interference or diffraction pattern is created when an object partially blocks the path from a monochromatic light source. Constructive interference occurs when there is a path length difference which is an integral multiple of the wavelength of the light from the source. When the obstructing object is a straight edge, the interference pattern will occur on one side only and caused by a path difference between light coming from a point source.

Lunar occultation is one such example of frequent and naturally occurring Fresnel diffraction by straight edge (Ghatak 2010). Since the astronomical sources are very far, they appear point-like and a small part of lunar limb acts as straight edge for the distant source. The intensity I at any distance x from geometric shadow for point source can be given by[1],

$$I = \int_{-\infty}^{x} exp\left(\frac{i\pi u^2}{L\lambda}\right) du \int_{-\infty}^{x} exp\left(\frac{-i\pi u^2}{L\lambda}\right) du \tag{1}$$

where λ is the wavelength of source light, x is the distance away from the edge, and L is the distance between the sight-line and the obstruction. In case of lunar occultation, L is taken as 384,000 km.

Above intensity equation for a point-like source is in integral form, and can be further simplified to derive relation of intensity as function of time and distance. The field E at a point in observer plane, corresponding to x, can be given by

$$E = \int_{-\infty}^{x} exp\left(\frac{i\pi u^2}{L\lambda}\right) du \tag{2}$$

The normalized intensity at any point is equal to $\left|\frac{E}{E_0}\right|^2$, E_0 is the value of the field observed without obstruction. When a broadband source is considered, the same intensity at two different wavelengths will appear at corresponding different distances x_1 and x_2 from the edge such that the field values E_1 and E_2 are results of similar interference. Here, x = 0 at all frequencies corresponds to the geometrical shadow, when the (point) source is on the Moon's limb. Considering this, the relation between distance and frequency f_1 and f_2 can be found out.

This would require $z_1 = z_2$, implying

$$\frac{x_1}{x_2} = \sqrt{\frac{\lambda_1}{\lambda_2}} = \sqrt{\frac{f_2}{f_1}} \tag{3}$$

The difference $\Delta x = (x_2 - x_1)$ between these distances (corresponding to same intensity feature, but at different frequencies) is thus

$$\Delta x = x_2\sqrt{f}_2\left(\frac{1}{\sqrt{f}_2} - \frac{1}{\sqrt{f}_1}\right) \tag{4}$$

From the above equation, it can be deduced that the spatial dispersion between two points on intensity curves is inversely proportional to square root of the frequency.

3. Temporal dispersion

In the above formulation, we have implicitly considered the obstruction to be stationary. For an occulting obstruction moving in a particular fashion, the resulting dispersion pattern will translate to temporal dispersion. In the following subsections, the dynamic spectrum for different relative motions of obstruction for both, point source and finite width source, are discussed.

3.1 *The velocity of obstruction is constant*

In order to get dispersion law in the fashion described usually for the ISM, the obstruction can be considered

[1] This particular form of expression is similar to that given by Richmond (2005).

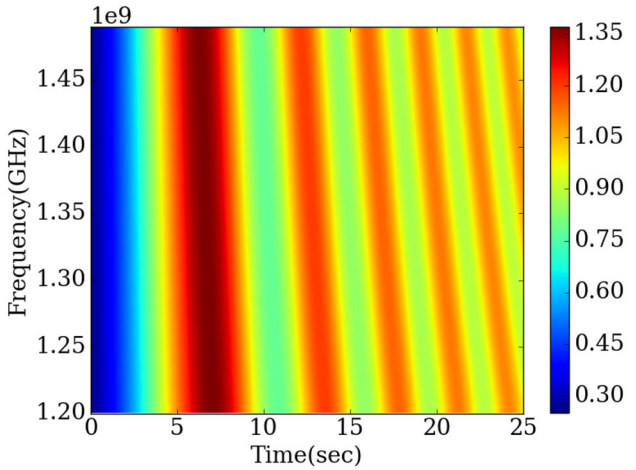

Figure 1. Intensity pattern of lunar occultation for a point source for uniform motion of the Moon.

to be moving with uniform velocity. The new formula associating time and frequency can be derived simply by dividing Equation 9 by constant value of velocity.

For the case of lunar occultation, the source (which is farther compared to the obstruction) is considered stationary. Hence, for the obstruction moving with velocity v m/s,

$$\Delta t = t_2 - t_1 = t_2\sqrt{f}_2\left(\frac{1}{\sqrt{f}_2} - \frac{1}{\sqrt{f}_1}\right) \tag{5}$$

where Δt is the time delay between same intensity feature observed at two frequencies. t_1 and t_2 are the associated time instants (measured from the time occultation began) at frequencies f_1 and f_2, respectively. It can be concluded from above equation, that as the time increases the dispersion delay also increases. Figure 1 is the dynamic spectrum simulated for lunar occultation for a point source with 1200 MHz to 1500 MHz frequency range. The dynamic spectrum shows that secondary fringes farther in time are more dispersed and less intense.

The motion of obstruction involves two cases, namely ingress and another is egress. These two cases follow different, in fact opposite dispersion trends. In order to make the effects clearly evident a very broad band of 1200 MHz to 3000 MHz is selected. Diffraction patterns in Figure 2 are for the motion of the Moon relating both ingress and egress. Considering center of lunar disk as origin, the negative and positive time indicates the time before and after the source crosses from left to right side of origin, respectively. The ingress shows negative dispersion in which a given intensity peak at a frequency appears to arrive earlier than that at the lower frequency. Far in the geometric shadow behind

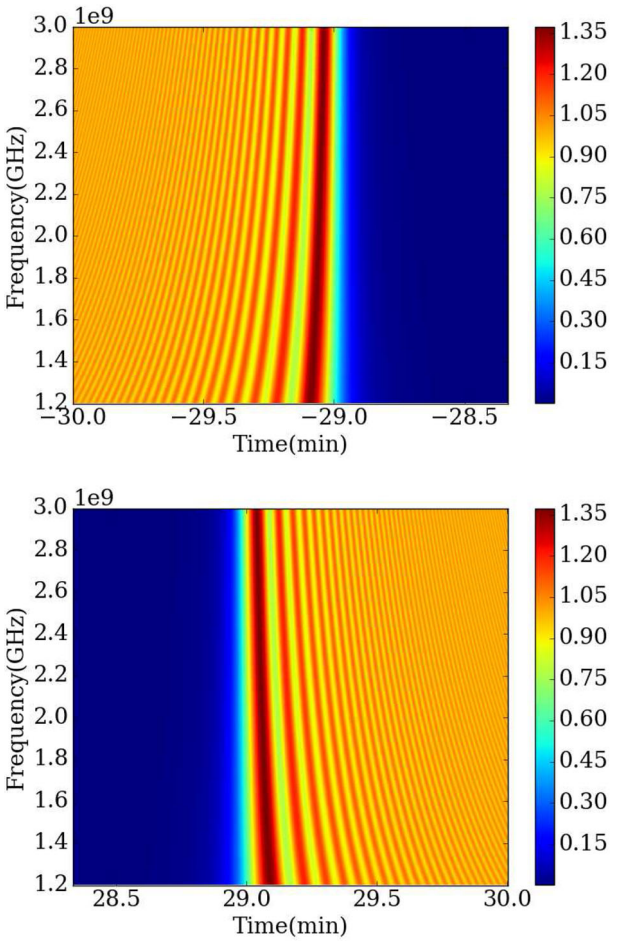

Figure 2. The dynamic spectra pre and post shadowing, wherein *negative* dispersion during ingress (top panel) and *positive* dispersion during egress (bottom panel) are clearly apparent.

the lunar disk also there is finite intensity but of microscale.

3.2 *Obstruction moving with uniform deceleration*

In order to explore if the ISM-like dispersion trend (for ISM, the time delay at a given frequency is proportional to inverse square of frequency) can be mimicked by diffraction, nonlinear motion of obstruction is considered. Constant deceleration is a common phenomenon which might be experienced by near earth asteroids, possibly large sized satellites due to drag forces in low earth orbit, or the objects moving in highly elliptical orbit. If an obstruction, moving with constant deceleration is considered, then with the appropriate parameters the ISM dispersion law can be achieved.

Let us assume the following time evolution of x,

$$x = x_0 + vt - \frac{1}{2}at^2 \tag{6}$$

where v and a are velocity and deceleration respectively. The roots of the above quadratic equation are

$$t = \frac{v \pm \sqrt{v^2 - 2a(x - x_0)}}{a} \tag{7}$$

$$t = \frac{v}{a} \pm \frac{v\sqrt{1 - (2a(x - x_0)/v^2)}}{a} \tag{8}$$

The second solution, after expanding the square root term using binomial expansion, and assuming $(x - x_0) = y$, may be expressed as

$$= \frac{v}{a}\left(\frac{1}{2} - \sum_{n=1}^{\infty}\binom{\frac{1}{2}}{n}\left(\frac{-2ay}{v^2}\right)^n\right) \tag{9}$$

In order to find the dispersion law followed by diffraction pattern under different situations, the following form is assumed with suitable units, so as to make it comparable with ISM dispersion law.

$$\Delta t(ms) = K * K_{DM}\big((f_1/(GHz))^{-\alpha} - (f_2/(GHz))^{-\alpha}\big) \tag{10}$$

Here, $K = 4.15\ (GHz)^{\alpha}$ ms, α is the power-law index, and K_{DM} is the proportionality constant equivalent to ISM dispersion measure (DM).

It is worth noting that, given the basic dependence $x \propto f^{-0.5}$, if we were to obtain the ISM-like dispersion law $t \propto f^{-2}$, we necessarily require $t \propto x^4$. We have explored a range of combinations of a,x,v and initial position in such a way that higher-order terms can be neglected, to see if we can get effectively a relation similar to that of ISM dispersion law. For example, if we take the distance to the obstruction as 6000 km, deceleration $a = 17.4\ \mathrm{m/s^2}$ and initial velocity 200 m/s, ignoring if these are or not realistic, then in the expansion as in Equation 14, the terms for $n \geq 5$ play insignificant role, and can therefore be neglected. In Figure 3, the time instants corresponding to the maximum intensity track sampled at different frequencies are plotted, assuming the above mentioned model parameters. In Figure 4, the top panel depicts the maximum amplitude of the band-summed feature (obtained after the otherwise dispersed *pulses* align maximally on *dedispersion*, following an assumed law), as a function of the trial α, the power-law index of frequency. The bottom panel of Figure 4 shows the corresponding optimal values of the proportionality constant K_{DM} as a function of α.

3.3 *Grazing occultation*

Here, we investigate a case in which obstruction grazes the source at some minimum distance x_{min}, as shown in Figure 5. With increasing distance x_{min}, the maximum intensity keeps decreasing, and approaches to a constant intensity. Essentially, the effect of obstruction gradually

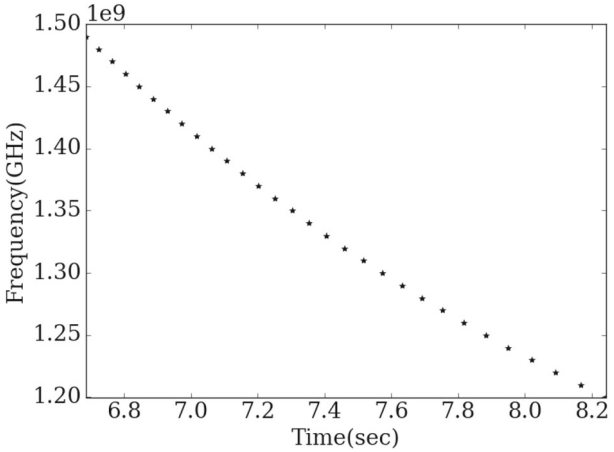

Figure 3. Dispersion of peak intensity points of first Fresnel lobe when the obstruction is moving with constant deceleration for 1200–1500 MHz band.

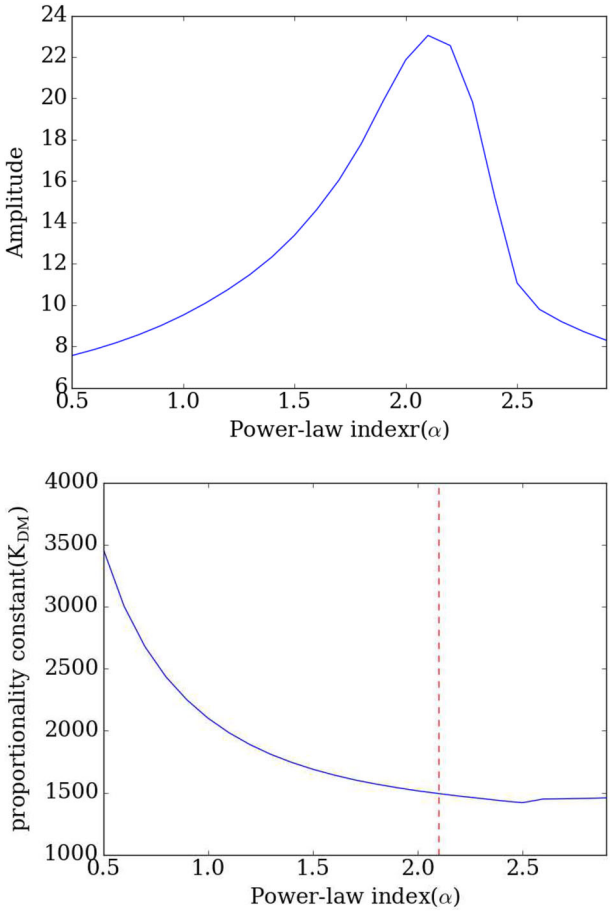

Figure 4. Dependence of amplitude of (band-summed) intensity (top panel), and the corresponding optimal proportionality constant K_{DM} (bottom panel), on the trial power-law index are shown. These refer to the case when effect of deceleration is included.

diminishes with increase in x_{min}. The dependence of distance x on time can be found out readily from the geometry as illustrated in Figure 5.

$$(x + R)^2 = (x_{min} + R)^2 + (v^2t^2) \tag{11}$$

or

$$x^2 + 2xR - (x_{min}^2 + 2x_{min}R + v^2t^2) = 0 \tag{12}$$

where R is the radius of lunar disk, and t is the time since closest approach. Solving the above quadratic equation, one of the solutions we get

$$x = -R + \sqrt{R^2 + (x_{min}^2 + 2x_{min}R + v^2t^2)} \tag{13}$$

Figure 6 depicts 4 cases of the dynamic spectra, as the minimum distance to obstruction is gradually increased.

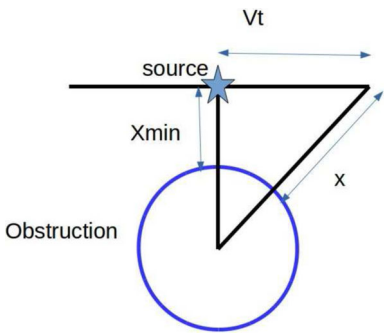

Figure 5. Source at some distance from obstruction.

It is evident from the plots that, as the minimum distance from the edge increases, the fluctuations in intensity decrease, and effects of diffraction vanish gradually. Here again, the distance and time are related to each other in nonlinear way. The factors which can affect the power-law dependence on frequency are the minimum distance, velocity and the radius of aperture/blockage. The dispersion found in this case does not resemble the dispersion due to ISM, for any of the explored combinations of parameters.

3.4 *Effect of angular size of the source*

So far, we have considered a point source occultation. However, the resultant diffraction pattern has multiple fringes. To closely relate to a single dispersed feature, we appeal to effects of finite source size. Unless mentioned otherwise, we assume for simplicity that the source angular structure (brightness distribution) is independent of frequency across the band being considered. When the apparent source size becomes bigger, the fringes get increasing washed out and the dependence on frequency changes gradually as we keep increasing the size of source. The dispersion delay between two points also gets reduced. If the source is large enough, then the secondary diffraction fringes vanish completely as shown in Figure 7. This can be probed by using

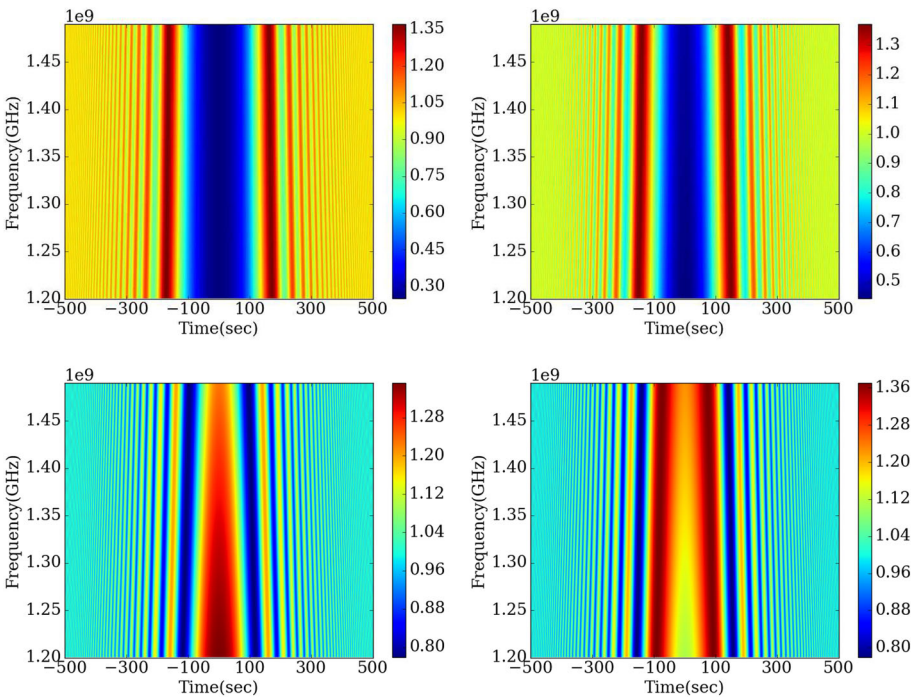

Figure 6. Source at different x_{min} distance from the edge, x_{min} increasing from top to bottom clockwise, with $x_{min} \sim 0$, 1, 3.2 and 4.8 arc-second respectively.

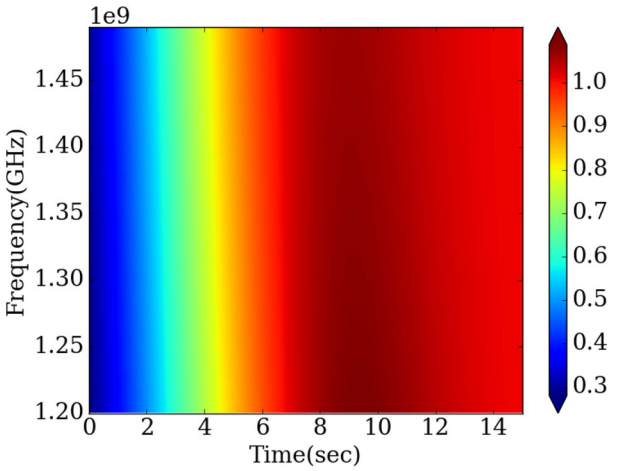

Figure 7. Dynamic spectrum for source size of $\sim$ 4.2 arc-second, wherein the higher order Fresnel lobes or fringes are washed out, as expected.

several different values of source size and finding the power index for reference points having same intensity.

From Figures 8 and 9, we summarize the result of this analysis, that as the size of the source varies, the relationship of relative time delay with frequency changes. As source grows bigger, the fluctuation in intensity diminishes as expected, but also does the relative time delay. The apparent net decrease in relative time delay, despite the increase in the power-law index, is to be understood as due to a more than compensating decrease in the DM-like proportionality constant, effectively reducing the dispersion-like effect.

4. Improvement in signal-to-noise ratio for large bandwidth

The effectiveness of lunar occultation to probe angular structure of the occulted sources hinges on high fidelity in measurement of the diffraction pattern at a chosen wavelength. The high fidelity implies the requirement not only of high signal-to-noise ratio in the measurements, but also of preserving the fine details in the apparent temporal pattern, or the so-called light curve. In radio astronomy measurements devoid of fine-scale spatio-temporal structure, the signal-to-noise ratio improvement is routinely sought by appropriate increase in one or more of the relevant parameters, such as the aperture area of the telescope, pre-detection bandwidth, and post-detection time constant (or integration) of the receiver. In contrast, the situation in occultation observations is rich in spatio-temporal structure that is also explicitly chromatic. This limits the

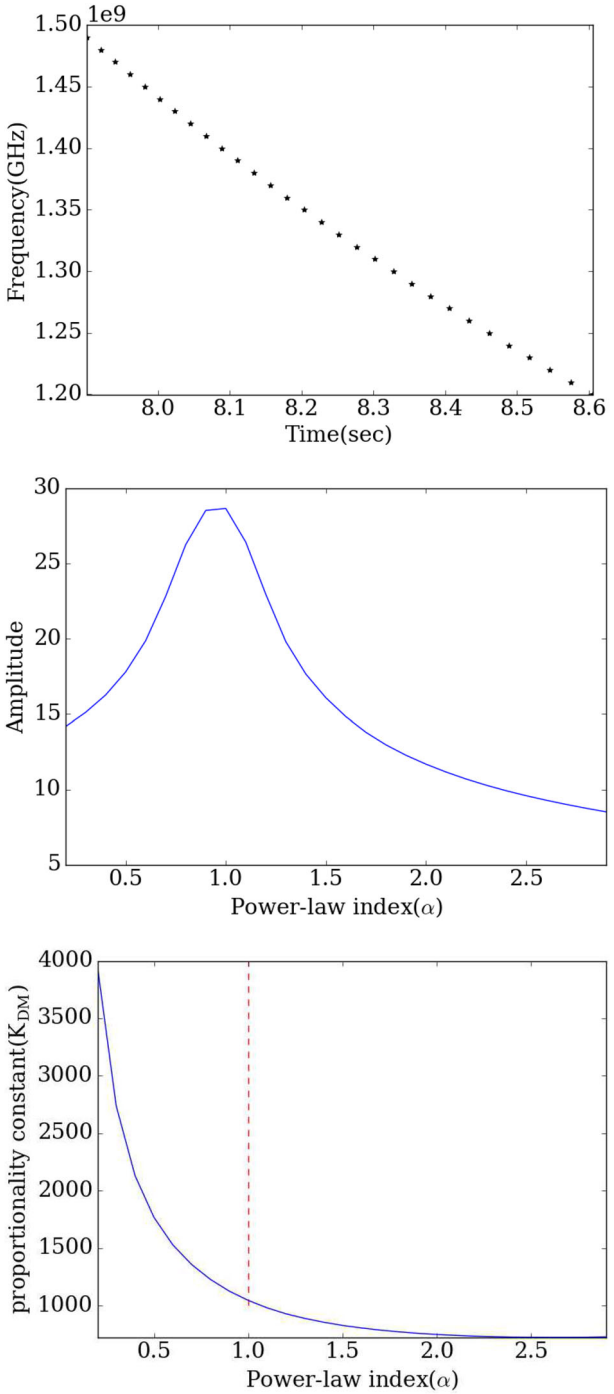

Figure 8. The top panel shows the apparent dispersion trend, wherein the times corresponding to the peak in intensity (in the light curves) shift systematically with frequency. The middle and the bottom panels show how the amplitude of the dedispersed pulse peak, and the implied DM-like proportionality constant (K_{DM}), respectively, vary as a function of the trial power-law index α. Here, the assumed source size is $\sim$ 3.2 arc-second.

potential improvements in the contrast against noise, in the occultation observations. Any increase in the above

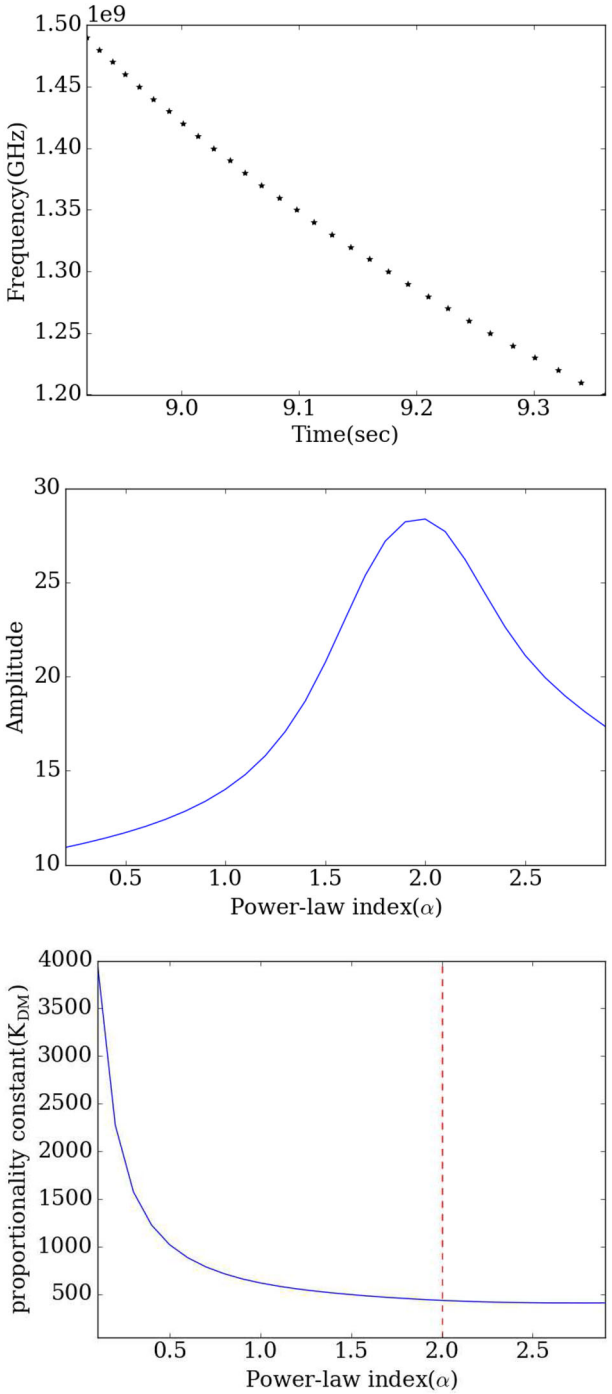

Figure 9. Similar to Fig. 8, but for source size $\sim$ 4.2 arcsecond.

mentioned parameters beyond their inherent scales in the occultation signal would wash out the related detail. These aspects have already been well-appreciated even at early times (for example, see Scheuer 1965) and optimum choices of the parameters and estimation method have been made where possible (see Singal 1987, and the references therein). In the following, we focus only on the chromatic nature of the occultation signature, and its implication for broad-band measurements. And as before, we assume, for simplicity, that the source structure (including its intensity) does not vary significantly across the observing band.

In the lunar occultation observations in the past, the resultant diffraction patterns observed and used for further analysis have invariably been the band-averaged versions, as far as we could find. As discussed also in the earlier part of this paper, the chromatic nature of the diffraction signature relating to occultation implies a well-defined spatial, and consequent temporal, scaling as a function of frequency. Hence, if light curves for a range of frequencies within an observing band are averaged without accounting for the chromatic effect, significant undesired smearing of the desired details in the light curve is inevitable. These details and their contrast (i.e. signal-to-noise ratio) are critical to deciphering the underlying source structure. While finite size/structure of sources also causes smearing in the apparent light curve, it is important to appreciate that here the smearing function is independent of the distance from the obstruction. To illustrate the effect of averaging over a bandwidth without correcting scaling effect, let us consider a point source and a finite size source observed at different bandwidths. The left panels in Figures 10 and 11 depict dynamic spectra of averaged diffraction pattern over different bandwidths for point source and for a source with finite diameter. It can be observed that there is more smearing of fringes when averaged over larger bandwidths. This smearing results in decrease in signal-to-noise ratio (SNR) and also, some of the details in the pattern are washed out, compromising the effective resolution and ability to decode the source structure.

In order to improve the SNR for wide bandwidths, while retaining the *fringe* contrast, suitable scaling correction for diffraction patterns at different frequencies can be made before directly averaging them across bandwidth. The scaling in time for point size sources follow the relation given in Equation 3. The equation can be used for correcting scaling effect by taking the scaling with respect to the center frequency as reference. After temporal-scaling correction, when diffraction patterns are averaged over bandwidth, the underlying signal contrast can be restored. The right-side panels in Figures 10 and 11 show spectrogram after such scaling correction. For finite size sources, it might appear that the averaging without scaling correction suffers relatively less deterioration in the intensity pattern than that for a point source. This is because some smearing

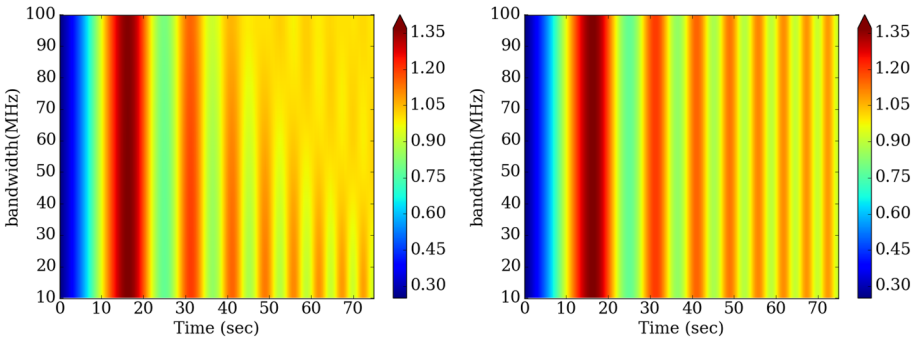

Figure 10. Above 2-D plot panels depict the band-averaged versions of Fresnel diffraction curve as a function of time and bandwidth. The left and the right panels represent band-averaging of diffraction curves for point source without and with frequency scaling correction, respectively. Despite the changing bandwidth, the center frequency of the bands is assumed to be fixed at 326 MHz.

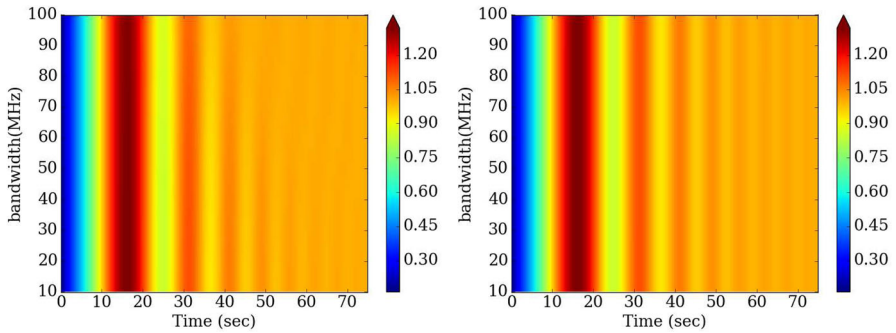

Figure 11. Similar to Fig. 10, but for a source size of about 2.5 arc-second (FWHM).

of the pattern is already caused by the finite source size. However, the scaling correction is required even in this case, for reducing the effect of *decorrelation* due to large bandwidth, which otherwise would be interpreted wrongly as due to source structure. The significant recovery in the fringe contrast as a result of the suggested correction is reassuring, and recommended. Alternatively, it is possible to consider appropriate model fitting path to decipher source structure from the observed dynamic spectra directly, since the dynamic spectral signature for a point source can be computed in detail readily. In the latter case, one can also relax the assumptions about the source structure being constant across the observed band. Thus, in any case, more sensitive probes using lunar occultation appear possible with use of wide bandwidths, offering sensitivity improvement proportional to square-root of the bandwidth, without degradation due to decorrelation of the patterns across the band. Such approach is now routinely feasible with the recent advance in sampling and analysis of wide-band signals to obtain dynamic spectral data with desired resolutions in time and frequency.

5. Conclusion and discussion

The study of lunar occultation across a broad band is conducted, computing and analysis, the dynamic spectra for the intensity pattern, as function of frequency and time. The intensity patterns show dispersion clearly, which increases as we move away from the edge of obstruction. The following five cases have been discussed.

(1) The velocity of obstruction is constant.
(2) Relative velocity is not constant.
(3) Grazing occultation.
(4) Apparent source size is finite.
(5) SNR considerations while using large bandwidth, and possible improvements.

The dispersion trend apparent in case of diffraction is very different from ISM dispersion law. Instead, the diffraction pattern shows spatial dispersion delay proportional to square root of frequency. While considering the first case, the dispersion characteristics of Fresnel diffraction remain unchanged due to uniform velocity of

obstruction. By introducing the non-linearity in relation between time and distance through non-uniform motion of obstruction, ISM like dispersion trend is achievable. But the considered scenario may not be physically realizable. The third case considered is the most probable and frequent situation, but doesn't display dispersion trend like ISM at all. In all above cases the occultation of point source has been considered. If the source has considerable angular width, the secondary fringes can be washed out and the dispersion trend closely follows ISM dispersion law. Although ISM like dispersion law is achievable under few circumstances and single pulse tracks are possible by considering effects of suitable angular size of the occulted source, but the narrowness of FRB pulses is not achievable in case of occultation. Also for every positive dispersion signature a negative counterpart preceding is unavoidable. Finally, as an independent discussion, the effect of bandwidth on SNR is considered, noting that diffraction pattern would be smeared when averaged across large bandwidth. The suggested way of doing scaling correction shows how the finer details lost due to bandwidth decorrelation can be recovered, while improving the SNR due to increase in bandwidth.

References

Ghatak, A. 2010, Optics, McGraw-Hill, 314–317
Hazard, C. 1976, Lunar Occultation Measurements, Elsevier (1976), 12(c), 92–117
Hazard, C. et al. 1963, Nature, 197(4872), 1037–1039
Lorimer, D. R. et al. 2007, Science, 318(5851), 777
Richmond, M. 2005, Diffraction effects during a lunar occultation, http://spiff.rit.edu/richmond/occult/bessel/bessel.html
Scheuer, P. A. G. 1962, Aust. J. Phys., 15, 333
Scheuer, P. A. G. 1965, MNRAS, 129, 199
Singal, A. K. 1987, A&AS, 69, 91–115
Swarup, G. et al. 1971, Nat. Phys. Sci., 230, 185
Von Hoerner, S. 1963, ApJ 140, 65